ISSN 0915-633X

NATIONAL INSTITUTE FOR FUSION SCIENCE

Conceptual Design of D-^{3}He FRC Reactor "ARTEMIS"

H. Momota, A. Ishida, Y. Kohzaki, G. H. Miley
S. Ohi, M. Ohnishi, K. Yoshikawa, K. Sato
L. C. Steinhauer, Y. Tomita and M. Tuszewski

(Received – July 3, 1991)

NIFS-101 July 1991

RESEARCH REPORT
NIFS Series

NAGOYA, JAPAN

CONCEPTUAL DESIGN OF D-^{3}He FRC REACTOR "ARTEMIS"*

H.Momota,
National Institute for Fusion Science, Nagoya 464-01, Japan
co-authored with
A.Ishida, Niigata University, Niigata 950-21, Japan
Y.Kohzaki, Institute for Future Technology, Tokyo 102, Japan
G.H.Miley, University of Illinois, Urbana, IL 61801
S.Ohi, Osaka University, Suita 565, Japan
M.Ohnishi and K.Yoshikawa, Kyoto University, Uji 611, Japan
K.Sato, Himeji Institute of Technology, Himeji 671-22, Japan
L.C.Steinhauer, STI Optronics Inc., Bellevue, WA 98004
Y.Tomita, National Institute for Fusion Science, Nagoya, Japan
M.Tuszewski, Los Alamos National Laboratory, Los Alamos, NM 87545

[ABSTRACT]

A comprehensive design study of the D-^{3}He fueled FRC reactor "ARTEMIS" is carried out for the purpose of proving its attractive characteristics and clarifying the critical issues for a commercial fusion reactor. The FRC burning plasma is stabilized and sustained in a steady equilibrium by means of a preferential trapping of D-^{3}He fusion-produced energetic protons. A novel direct energy converter for 15MeV protons is also presented. On the bases of a consistent scenario of the fusion plasma production and simple engineering, a compact and simple reactor concept is presented.

The design of the D-^{3}He FRC power plant definitely offers the most attractive prospect for energy development. It is environmentally acceptable in view of radio-activity and fuel resources; and the estimated cost of electricity is low compared to a light water reactor. Critical issues concerning physics or engineering for the development of the D-^{3}He FRC reactor are clarified.

"Keywords" D-^{3}He, FRC, Conceptual Design, Power Plant, Fusion Reactor

---

* Supported by: a Grant-in-Aid for Fusion Research from Japanese Ministry of Education, Science and Culture, by a cooperative program of the National Institute for Fusion Science, and by the "Lunar Base and Lunar Resources Associate" : U.S.-Department of Energy; discussed at a series of the U.S.-Japan cooperation on D-^{3}He in Field-Reversed Configuration.

1. Introduction

Progress in fusion research has been achieved mainly on tokamak experiments, and a scientific feasibility experiment will be performed before long on this concept. Nevertheless, a number of engineering problems have to be resolved before D-T fueled tokamaks become accepted as commercial fusion reactors. Development of a reasonable tritium breeding blanket is one such example. Among those, certain engineering problems for a commercial D-T fusion reactor are attributed to 14MeV neutrons, which seem very hard to resolve.

14MeV neutrons cause damage of the structural materials of the blanket. Embrittlement of the materials shortens their life, which has been estimated[1,2] at less than 10MW*Year/m^2. It is preferred, therefore, to develop certain materials which retain their characteristics in a 14MeV neutron environment as long as 100MW*Year/m^2. Disposal of a large amount of radio-activated wastes is also the big problem for the ecology of the environment because it takes more than several tens of years before the decay of induced radio-activity to an inappreciable level. Further, reasonable costs of electricity or high plant efficiencies of reactors are required for commercial power plants. In a conventional D-T fusion concept, 80% of the fusion energy is carried by 14MeV neutrons to the blanket and then the heat energy is converted into electricity through turbines and generators. The overall plant efficiency is therefore limited to the low level of turbine-generators.

Deuterium and helium-3 fusion fuels are considered to mitigate these engineering problems associated with 14MeV neutrons. With those fuels, the fraction of 14MeV neutrons in the total fusion power decreases to a few percent[3,4] and more than 70% of fusion power can be conducted[3] to direct energy converters, which enable us to achieve a highly efficient fusion plant. Physics requirements such as the confinement parameter $n\tau$ and the operation temperature T needed to sustain D-^{3}He fusion reactions are as high as 10^{21}sec/m^3 and around 100keV, respectively. A large plasma beta-value (>30%) is also recommended so as to reduce a synchrotron radiation loss and to obtain consequently a higher plant efficiency. Accessibility of high-power direct energy

converters is necessary to utilize the power carried by charged particles.

By its intrinsic characteristics a field-reversed configuration (FRC) seems to meet the above requisites. The plasma is confined by closed lines of force for good confinement and surrounded by open lines of force for charged particles extraction. Since an FRC has no toroidal magnetic field for plasma stability, a stably confined FRC plasma so far obtained in experiments[5,6] has an extremely high beta value (>50%). On this background, preconceptual designs of D-^{3}He FRC fusion reactors have been carried out. One is very small, pulse-operated reactor concept "SAFFIRE"[7]; whose small size might be favorable for stability, but is unfavorable for obtaining a high plant efficiency. The other is a 1MWe stationary operated reactor concept "RUBY"[8]; which contained many unresolved problems in physics and engineering, especially in the area of plasma stability.

An FRC is experimentally stable against macroscopic tilt modes unless its s-value (the ratio of plasma radius and averaged gyroradius of ions) is much larger than unity. If the s-value is not so large, a certain stabilization effect[9] is expected by employing a large elongation of an FRC. Since the s-value is proportional to the trapped magnetic flux Ψ as well as the separatrix radius, a representative s-value for a few gigawatts D-^{3}He FRC reactor is much larger than unity. Thus, one must employ a stabilizing method which will be effective in commercial fusion plants with a large s-value. Stabilization by energetic charged particle beams[10] in a large s FRC has been demonstrated, analytically for rigid tilt modes[11] and numerically for full tilt modes[12]. One possibility of supplying the beam is the injection of energetic neutral particles. In a D-^{3}He burning plasma, however, the preferential trapping of fusion protons serves as an energetic particle beam which stabilizes tilt modes and also provides a major part of the seed current needed to sustain an FRC plasma in a steady burning equilibrium.

A conceptual design study of this D-^{3}He FRC fusion reactor "ARTEMIS" has been carried out for the purpose of examining its attractive characteristics and clarifying the critical issues for commercial fusion reactors. The design retains the essential features of "RUBY" and modified it so as to describe a complete scenario of the plasma by making use of the stabilization effects due to energetic beam particles.

It should be noted that a significantly different D-^{3}He fuel fusion reactor "APOLLO[13]" has been studied based on a low-beta tokamak. Since in that design more than 90% of the fusion energy is carried by radiations, highly efficient rectifying antennas are needed. It appears that the D-^{3}He fuel enables the reactor to be inherently safe and the first wall to be permanent during the life of the reactor.

An overview of the "ARTEMIS" reactor design is presented in the next Section 2. Parametric studies on D-^{3}He fusion plasma are described and principal parameters of a steady equilibrium of a burning plasma are fixed in Section 3. In Section 4, a start up scenario of FRC plasma to the D-^{3}He burning state is discussed. This is achieved by a compression of the external magnetic field, fuel injections, and neutral beam injections of energetic particles. One of the key technologies of "ARTEMIS" design is direct energy conversion. In this design, we introduce a novel traveling wave direct energy converter which is introduced in Section 5. In Section 6, we verify the attractive characteristics of D-^{3}He FRC reactor "ARTEMIS" by estimating the cost of electricity and find that the reactor is economical compared to a light water reactor. The last section (Section 7) is devoted to discussions of the results and to critical issues for further studies.

2. Overview of "ARTEMIS" Reactor Concept

The D-^{3}He fueled FRC fusion reactor "ARTEMIS" consists of a formation chamber, a burning chamber, and a pair of direct energy converters all of which are connected by the magnetic lines of force (Fig.1). An FRC plasma is produced at the start by the conventional reverse-biased fast theta pinch method in the formation chamber and then translated to the burning chamber. A combination of neutral deuterium beam injection (NBI), fueling, and a slow magnetic compression in the burning chamber brings the volume, the temperature, and the number density of the plasma up to those for the D-^{3}He burning state. The bulk of the D-^{3}He fusion energy is carried by charged particles along the lines of force, which connect to a pair of direct energy converters. A smaller fraction of the fusion energy is carried by neutrons and photons to the first wall of the burning chamber. This energy is

converted to electricity by turbine-generators.

[Fusion Plasma]

The formation chamber is arranged symmetrically so as to reduce error fields to a level as low as possible. Therefore only a small port for gas puffing is installed in a symmetric coils and vacuum chamber system. Then, reliable FRC plasma formations can be achieved even for a very low feeding gas pressure. A fast rising theta-pinch discharge with a one turn voltage of 400kV in a filling gas pressure of 0.05Pa and bias field of 0.035T produces an initial FRC plasma whose parameters are listed in Table 1-a. The plasma is then translated to the burning chamber due to an unbalanced cusp magnetic field. During the translation, the FRC seems to conserve particle numbers of respective species, the total energy, the trapped flux, and its "Intelligence". Plasma parameters obtained in this way at the burning chamber are listed in Table 1-b.

In the burning chamber, the FRC plasma is heated by means of energetic neutral deuterium beam injection, whose maximum power is 100MW, and fueled by injecting D-^{3}He ice pellets. A slow magnetic compression is also applied. The injected particles form an ion beam current which plays a roll of the seed current needed to sustain or increase the trapped magnetic flux of an FRC. The plasma evolves in its volume, the density, and the temperature for a burning plasma. During the evolution, the ratio of the current carried by the energetic beam particles to the total plasma current is high enough to stabilize an FRC against macroscopic modes. A set of plasma parameters obtained in this way are tabulated in Table 1-c.

In a D-^{3}He burning FRC plasma, a current drive due to the preferential trapping of fusion protons assisted by a small amount of external beam injections is sufficient to sustain an equilibrium in a steady burning state[14]. The particle flows in this steady burning D-^{3}He FRC plasma are exhibited in Fig.2, where the particle transport is assumed to be 206 times the classical rate[15].

[Key Technologies]

A fairly low feeding gas pressure of 0.05Pa and a high one-turn voltage of pinch coils are needed to obtain an FRC with a low s-value. Insulation for this high voltage is achieved by

applying a 4-stage tandem structure of the pinch coils.

Pulse SC coils of 1.87MAT/coils at the formation chamber raises the magnetic field up to 1.26T in a period of 50msec. Fast coils for this compression (25T/sec, max.1.26T) are ready to perform with the present technology, since a fast rising super-conducting coil which gives a rising rate of 200T/sec and a maximum field of 4T has been examined[16] with a 3-staged strand cable. A large radius, 5m, is chosen for the compression coils in order to reduce the coupling with the coaxial pinch coils, 2.1m radius, with an assist of a magnetic shielding plates.

The development of pellet acceleration is one of the most important engineering problems in fusion research: a representative speed of a pellet needed to inject a pellet deeply into a plasma center is several times 10^4m/sec, which may be compared with a presently available speed: 10^3m/sec. In "ARTEMIS" design, however, a pellet of 1.8mm^3 volume consists of an ice deuterium vessel and inner liquid helium-3 is dropped every 0.9 seconds. At the moment, FRC plasma displaces with the aid of an applied cusp field towards the pellet at the speed more than 10^4m/sec and consequently swallows it deeply inside the plasma.

A set of 10 super-conducting coils of 14.2MAT/coils and radius of 3.5m is installed at the burning chamber and supplies a magnetic field of 6.7T. The required averaged current density of 30A/mm^2 is conventional and the stress of 300MPa is easily held by a reinforced structure of strand cable.

For the purpose of heating the plasma as well as driving plasma current which is needed to sustain the plasma in a steady equilibrium, injections of 1MeV deuterium neutral beam particles are employed. The maximum power of 100MW is required for the start up and 5MW to sustain the plasma in the steady burning state. The development of this neutral beam is presently within the scope in R&D programs for ITER.

One of the most important technologies to be developed for a D-^{3}He FRC reactor is the direct conversion of fusion power carried by charged particles. For the thermal component of a plasma, a "Venetian blind type" generator[17] (VBDEC)" might be applicable. For 14.7MeV fusion protons, however, the energy is too high to maintain the necessary electrical insulation. The concept of a "traveling wave direct energy converter[18](TWDEC)" is developed based on the principle of a "Linac"[19].

[Reactor System]

Following the above discussions, a conceptual design of D-^{3}He FRC power reactor "ARTEMIS" has been carried out, whose power flow chart is exhibited in Fig.3. All of the technological bases employed for this design are conventional. A conversion efficiency of heat energy to electricity is assumed to be 36%. Owing to the high efficiencies of direct energy converters, the overall plant efficiency is estimated as high as 62%. The principal parameters of the plant are shown in Table 2. The device is consists of straight tubes forming a linear geometry and is consequently easy to disjoint for maintenance.

On the bases of the ESECOM study[20], costs of electricity have been estimated. The total weight of the reactor, excluding NBI, is approximately 3,300tons which is 1/3 of a corresponding light water reactor. Table 3 summarizes the costs of electricity (COE) for the D-^{3}He FRC reactor "ARTEMIS". An average load factor of 75% is assumed. It must be noted that the fuel cost (assumed cost of helium-3 obtained from the Lunar soil[21] of 0.2M$/kg) contributes only 4%. The estimated COE is 28.7mills/kWh from "ARTEMIS", which is cheaper than the estimated COE: 33.4-56.6 mills/kWh[22] from a presentday light-water reactor.

3. D-^{3}He Fusion Plasma

The favorable characteristics of D-^{3}He fusion fuels follow from their small amount of 14MeV neutrons and higher radiation parameter (the fraction of the power introducible to direct energy converters to the total fusion power). On the other hand, the required ignition product $n_e\tau_E T$ is 25 times larger than that of D-T fuels. The 14MeV neutron power fraction (the ratio of the power carried by 14MeV neutrons to the total fusion power), the radiation parameter, and the triple product $n_e\tau_E T$ for ignition are exhibited respectively in Figs.4-a, 4-b, and 4-c versus the concentration of helium-3 and deuterium, where a plasma temperature of 90keV and an average beta-value of 90% are assumed. The ratio of the particle confinement time and the energy confinement time is also assumed to be 2. The radiation loss increases through an enlargement of effective Z, and 14MeV neutron fraction decreases as the fuel ratio increases. On the bases of these calculations, we will employ a density ratio

between helium-3 and deuterium to be 1/2, which maximizes the radiation parameter and minimizes the required ignition product $n_e \tau_E T$.

The characteristics such as the 14MeV neutron fraction, the radiation parameter, and the confinement parameter $n_e \tau_E$ for ignition of D-^{3}He fusion plasma change as the operation temperature changes. Figures 5-a, b, and c describe respective values versus the operating temperature. Averaged beta-value is still assumed to be 90%. The particles confinement is assumed to be a twice of the energy confinement time. Observe in Figs.4 and 5 that the D-^{3}He plasma temperature of 70keV-100keV and the concentration of helium-3 density of 0.4-1 times the deuterium density are recommended to obtain a favorable fusion plasma. We will choose a plasma with a temperature of 87.5keV and a helium-3 density of one half of the deuterium density. It must be noted that elastic nuclear scattering of energetic particles are ignored in these calculations. It is expected that the 14MeV neutron fraction and the required triple product will decrease and the obtained radiation parameter increase once elastic scattering is taken into account.

In a D-^{3}He burning FRC plasma, the momentum transfer from a directed flow of fusion particles causes a rotation of the background fuel plasma around the axis of symmetry. Consequently the conventional analysis for obtaining an equilibrium by solving the Grad-Shafranov equation is no more applicable. We developed, therefore, a reasonable method[23] to obtain a steady state equilibrium of burning FRC plasma: to solve a set of equations for respective species of the fuel plasma describing the static balance between inputs and losses regarding to particle numbers, momenta, and energies. The equilibrium is then obtained in terms of inputs of particles, momentum, and energy. A solution at the midplane obtained for this design is exhibited in Fig.6: the magnetic field in Fig.6-a, the electron density in Fig.6-b, and the rotation velocity in Fig.6-c. A uniform distribution of the plasma temperature, as is normally observed in experiments, is assumed. Microscopic turbulence was also introduced so as to causes an anomalous transport factor of 206. The total current for an FRC is estimated as 160MA for a separatrix radius of 1.12m and a plasma length of 17m. The seed current of 50MA is needed to sustain the plasma in the steady state equilibrium. Since the plasma temperature is very high and consequently the slowing down

of an energetic particle is very small, the seed current of 50MA is obtained by injecting steadily 1MeV beam particles of an effective current 22A. Fortunately, an appreciable amount of this seed current (42MA) is naturally supplied in D-^{3}He burning FRC plasma by the proton beam arising from the preferential trapping of 14.7MeV fusion protons. Consequently, the injection of 1MeV beam particles whose current is less than 5A is enough to sustain the plasma in the steady burning equilibrium.

A set of plasma parameters obtained in this manner is listed in Table 4. For a plasma temperature of 87.5keV, a concentration of fuel component $n_{^3He}:n_d=1:2$, and an electron density of $6.6*10^{20}/m^3$, the required energy confinement time τ_E is 2.1sec. Observe that 74% of the fusion power is carried by charged particles. The plasma volume and input power is as small as $67m^3$ and 5MW, respectively. These characteristics result in a highly efficient power plant using D-^{3}He fuels in an FRC.

In the D-^{3}He burning FRC plasma, tilt modes may be stabilized by energetic beam particles as was demonstrated by Barnes and Milroy[12]. The beam current must exceed 20-25% of the total current for stabilization by this means. Further, rotational modes may also be stabilized[24] with the aid of a beam current of only a few percent of the total current. A particle beam current of 27.5% of the total current is regarded as sufficient to stabilize all macroscopic modes.

4. Start up of the Fusion Plasma

An FRC plasma is first formed at the formation chamber where a set of 7 pinch coils, a set of 8 fast coils, and two pair of cusp coils are installed. A cross-sectional drawing of the formation section is shown in Fig.7. Coaxial fast coils are magnetically shielded from the pinch coils so as to avoid an induced high voltage. Each pinch coil has a 4-stage tandem structure which forms a series circuit with power sources, as is illustrated in Fig.8. A bias field of -0.035T together with the two cusp coils yields cusped magnetic field structures at both ends of the device. A fast acting gas puff for feeding 52mPa of D_2 and ^{3}He mixed gas and low voltage circuits of the pinch coils are activated at the time t=-1 msec, and then the high voltage circuits are closed at the time t=0. At the time t=5msec, the current

in fast SC coils starts to rise rapidly to supply the guide magnetic field which connects the burning chamber and the direct energy converter. The representative characteristics of pinch coils and fast SC coils are listed in Table 5, together with slow SC coils at the burning chamber. The gases are ionized and compressed until t=4.8μsec. The plasma expands for the following 0.7μsec and the formation of an FRC plasma is completed. The plasma is then compressed adiabatically as is seen in Fig.9. The obtained parameters of the FRC plasma was listed in Table 1-a. After completing the formation of a field-reversed configuration, the plasma is translated by applying unbalanced cusps toward a magnetic bottle at the burning chamber.

The number of confined particles for respective species, the total energy, and the trapped magnetic flux in the FRC are conserved during the translation because the duration of the translation is much smaller than the characteristic times of dissipations. This condition determines the plasma parameters just after the translation as was exhibited in Table 1-b.

In the burning chamber, the FRC plasma is heated up by means of injected energetic beam particles whose maximum total power is limited to 100MW, which also provides a seed current and consequently sustains or enhances the trapped flux of the FRC. D-^{3}He pellets are also injected to resupply the fuel and an applied external magnetic field is raised from 0.22T to 6.7T for 50sec. A cross-sectional drawing of the burning section is given in Fig.10, where eight ports for neutral beam injections and a port for pellet injections are installed. The temporal values of an applied external magnetic field, the input NBI power, and number of the injected particles, respectively, are shown in Fig.11-a, b, and c. Parameters of the plasma such as the plasma temperature T, the plasma radius r_s, and the plasma length l_s develop in accordance with the continuity of particle species, the energy conservation, and the force balance. Both the particle transport with a temperature dependent anomalous multiplier of $10+0.244*(T/1kev-1)^{3/2}$ to the classical one and the energy transport of twice the particle transport are assumed. The consequent development of the plasma is shown in Fig.12-a, b, and c. At the time t=50sec, the plasma parameters attain the values required for D-^{3}He burning. Since the ratio of the current carried by energetic particles to the total current exceeds 0.25 during the development, the FRC plasma should be stable. In this way, we have a

burning FRC plasma whose representative parameters are listed in Table 4.

5. Direct Energy Conversions

Since a large amount of fusion power is carried by charged particles in a D-^{3}He burning FRC reactor, a use of highly efficient direct conversion of the energy into electricity is recommended to achieve an attractive fusion power plant. The application of direct energy converters in a plasma device is often a serious problem, since a fairly large area of ion collector plate might be required to decrease the input power density and to remove the heat reasonably. Fortunately an FRC plasma is surrounded by open lines of force and thus is suitable for the application of direct energy converters.

The fusion power carried by charged particles consists of 810MW of thermal ions and 368MW of 14.7MeV protons in the "ARTEMIS" design. The energy spectrum of the former includes the thermal spread of 420keV with a biased energy of $Z_j e\phi$, where Z_j is the charge number of the ions specified by the subscript j and ϕ=135kV is the ambipolar potential attributed to a prompt loss of electrons along lines of force. Note that these values are consistent to our assumptions i.e., τ_n/τ_E=2. Recalling[25] that the flashover voltage V(kV) is between $35*g^{0.5}$ and $35*g^{0.6}$ in a hydrogen atmosphere of less than 0.1Pa where g is the gap length in mm, one is able to decelerate a majority of thermal ions with the use of a DC voltage and a reasonable gap length. In our design, Venetian blind type direct energy converters (VBDEC) with 5-stage fin arrays are employed to obtain a higher conversion efficiency. Examples of ion orbits in the direct energy converter are exhibited in Fig.13; and the size and the applied voltage of the ion collector for respective stages are listed in Table 6. The 2m radius and 2.2m length of the assembly are enough to recover the energy of the thermal component with a efficiency of 60%.

A pair of traveling-wave direct energy converters (TWDEC) are installed at both downstream ends of the VBDECs. These are designed to convert the kinetic energy of 14.7MeV protons whose energy is too high to control by an electrostatic potential. Each converter consists of two parts: One is the modulator which

modulates the velocity of 14.7Mev proton beam by an electrostatic propagating sawtooth wave whose wave length is λ_0 and the applied maximum potential is V_m. The phase velocity of this wave is chosen to be the same as the velocity V of 14.7MeV protons, i.e.,$5.3*10^7$m/sec. Then the proton beam is modulated and focussed at $x_f = (\lambda/4)*(14.7MeV/eV_m)$ measured from the downstream side of the entrance of the modulator. The other is a decelerator where a set of mesh grids with an entrance at $x=x_f$ provides a traveling electrostatic wave $V(x,t) = V_d\cos[\int_x k(\xi)d\xi-\omega t]$. The bunched 14.7MeV protons are trapped in a phase ϕ of the wave, provided that the phase velocity of the wave is close to the velocity $5.3*10^7$m/sec at the entrance. The phase velocity of the applied traveling wave is decreasing with a decreasing gap distance of the grids in the direction of the beam so as to lower the energy of the protons to the range suitable for VBDECs.

The focus of the proton beam is spread, however, due to a thermal spread of fusion protons. The spreading of the focus spoils the trapping of the protons within the traveling wave and eventually lowers the efficiency of TWDEC. In order to examine the trapping and deceleration of the fusion protons, particle trajectory calculations were carried out, one of which can be seen in the phase space plots of Fig.14. A wave-length of 4.7m was employed for the modulator and the entrance of the decelerator. By applying the maximum voltage V_m of 0.82MV to the modulator, the fusion protons are bunched and then trapped around a phase $\phi = 5\pi/6$ behind the peak of the applied traveling wave potential whose maximum voltage V_d=0.42MV. More than 95% of the 14.7MeV beam protons are trapped during the deceleration, however, a certain fraction of protons once trapped will be lost through collisions with the mesh structure of the grids.

The assembly of the traveling wave direct energy converter consists of 24 mesh grids,i.e., 5 for the modulator and 19 for the decelerator, and located as is shown in Fig.15. Each mesh grid is made of water cooled SUS pipes of 17mm diameter and 1mm thickness and arranged with a distance of 1.3m. A pressure difference of 5MPa is applied to cool the pipes and the stress due to pressurized water is 40MPa, which is much smaller than the allowable limit for this pipe. The total power needed to cool the grid is estimated as 140kW. The energy flow in the traveling wave direct energy converter of this structure is exhibited in Fig.16. The total flux of 14.7MeV protons is 183MW or

$7.8*10^{19}$/sec into a TWDEC. A power of 131MW is extracted with a set of mesh grids and a power of 12MW is carried to the end collectors where 5.9MW is collected as electricity. Thus the total efficiency of TWDEC for fusion protons is approximately 75%.

6. Evaluation of D-^{3}He FRC Reactor "ARTEMIS"

We will attempt to evaluate D-^{3}He FRC reactor "ARTEMIS" for the purpose of clarifying its favorable characteristics and indicating the optimum direction of the development. In estimating various energy systems or conceptual designs, it is important to compare these systems with an unified standard which allows a wide range of variations. Comparisons of this type have been made in the United States and a frame of estimating the standard cost of fusion reactors, light-water reactors, advanced fission reactors, and various power plants has been devised. An assessment of the competitive potential of magnetic fusion energy compared with present and future fission energy sources has been completed by the Senior Committee on Environmental, Safety, and Economic Aspects of Magnetic Fusion Energy (ESECOM).

The base of calculating the cost of electricity with the D-^{3}He FRC reactor "ARTEMIS" is to estimate the mass of components presented in the design and integrate them after multiplying the unit cost ($/kg) which is also given by the ESECOM standard. For the cost of an components whose engineering base is the same as a certain conventional components, however, we introduced appropriate scaling rules. A summary of the total plant capital cost is presented in Table 7. The following assumptions have been made,i.e., interest during construction = 0.0856, plant life time = 30years, and indirect cost factor = 0.581. The cost of fuel for the ARTEMIS reactor is assumed to be 0.2M$/kg, roughly twice that assumed in the ESECOM study. In this Table, one finds that the total mass of the reactor is as small as 3,300tons which is 1/3 of the primary system of an equivalent light-water reactor and one order of magnitude smaller than that from an equivalent D-T tokamak reactor design. This is brought from the fact that the FRC plasma is compact and the plant efficiency is as large as 62%. The small amount of the total mass results in a small total capital cost of the plant.

On the bases of these cost analyses, the cost of electricity (COE) is estimated (Table 3), i.e., 28.7mills/kWh. The COE is to be compared with that from a D-T tokamak reactor design or that from light-water reactors. The cost of fuel helium-3, which we assumed to be obtainable from lunar surface by 0.2M$/kg, accounts for only 4% of the COE. For the case of increased fuel cost, e.g., 1M$/kg, the increment of COE is only 17%.

A confinement anomaly factor of 206 is assumed for the burning state of this design. For the case of a larger anomaly factor, the size of the fusion plasma is increased so as to meet the requirement for the confinement parameter $n_e \tau_E = 1.38*10^{21}$ sec/m^3. A limiting factor for increasing the size may be the stress of the magnetic coils, less than 300MPa from ARTEMIS design, which is much lower than a estimated limit 800MPa. Another important factor may be the wall load of 14MeV neutrons. The wall load of 0.27MW/m^2 from the ARTEMIS design enable the life of the first wall to exceed the life of the reactor, i.e., 30years. For an anomaly factor of 1000, magnetic field should be changed by 5.3T and size of the reactor should be larger by a factor 2.8. Then both the maximum stress of the coils 300MPa and 14MeV neutron load onto the fist wall 0.27MW/m^2 is unchanged. The net output power changes, on the other hand, to several GW_{net}. Thus the large technological flexibility of the D-^{3}He fuel FRC reactor enable the design to meet large varieties of unknown parameters.

Other area where the D-^{3}He ARTEMIS power plant has very attractive characteristics might be the safety and environmental features compared to D-T fusion power plants. Since the 14MeV neutron yields are 0.01 to 0.017 times of that from an equivalent D-T power plant, the ARTEMIS structure can be disposed of as low-level wastes after a full reactor lifetime. Analyses on the decay heat and on the storage of the tritium inventory are areas that need to be researched. Nevertheless, because of its small neutron yields and its small tritium exhaust of 8.6mg/min, the inherent safety of ARTEMIS power plant is evident.

7. Summary of the Results

A conceptual design of a D-^{3}He fuel FRC fusion reactor "ARTEMIS" is carried out. An FRC is chosen to confine D-^{3}He burning

high beta plasma since it is surrounded by open field lines suitable for installing high power direct energy converters to extract the major part of fusion energy. By the choice of an FRC, a very compact fusion plasma and linear geometry of the reactor, which is convenient for disjointing and repair of the reactor, are gained. This configuration contrasts with that of a D-^{3}He tokamak, where the volume of the plasma is fairly large and the major part of fusion energy is carried by radiation.

An important role for energetic beam particles is adopted in the ARTEMIS design. These beam particles stabilize an FRC plasma from tilt modes as well as rotational modes. Further, they drive the plasma current needed to develop and to sustain the plasma in a steady burning equilibrium. In a D-^{3}He FRC reactor, the energetic beam particles are supplied by an NBI during the pre-ignition phase and by a preferential trapping of fusion protons in an FRC during the steady burning phase. Thus, a D-^{3}He FRC appears to be attractive with respect to stability as well as the sustainment of the equilibrium in a steady state. The stabilization effect attributed to energetic beam particles is one of the most important areas that should be examined in experiments.

The concept of a traveling wave direct energy converter is developed to extract the fusion energy carried by 14.7MeV fusion protons. The technologies needed for this development are conventional. The life time of existing structural ferritic steels are as long as the total reactor life of the ARTEMIS and no development of new materials is necessary. Fuel injection is simple with the moving FRC method. Operation of large and extremely high field magnetic coils is not required. Thus the bases of technologies employed for ARTEMIS design are conventional and have large technological flexibility which enable the design to accommodate large varieties of unknown parameters. Optimization studies and engineering developments of direct energy converters as well as highly efficient negative ion beam sources are needed before starting high power operation of the experiment.

The estimated COE from ARTEMIS is approximately 30mills/kWh which is cheap compared to a light water reactor or a tokamak reactor. Dependence of the fuel cost on COE is very weak. The very small radioactivities, low tritium yields, and the inherent safety of the power plant might be acceptable socially and ecologically. Thus the characteristics of a D-^{3}He fuel FRC fusion

power plant definitely indicate the most attractive prospect of the energy development for the 21st century.

[REFERENCES]

1) G.L.Kulcinski; IAEA CN-33/S-3-1 (Held at Baltimore, 1977)
2) R.W.Conn; Journ. Nuclear Materials vol.76&77 (1978) 103
3) H.Momota, et al.; Nuclear Inst./Meth. in Physics Research vol.A271 (1988) 7
4) W.Kernbichler and M.Heindler; Nuclear Inst./Meth. in Physics Research vol.A271 (1988) 65
5) R.E.Siemon, et al.; Fusion Technology vol.9 (1986) 13
6) M.Tuszewski; Nuclear Fusion vol.28 (1988) 2033
7) G.H.Miley, et al.; Electric Power Institute ER-645-1 (1979)
8) W.Kernbichler, et al.; IAEA CN-53/G-2-3 (Held at Washington DC, 1990)
9) L.C.Steinhauer and A Ishida; Physics of Fluids B vol.2 (1990) 2422
10) C.Mehanian and R.D.Lovelace; Physics of Fluids vol.31 (1988) 1681
11) Y.Nomura; Journal Phys. Soc. Japan vol.54 (1985) 1369
12) D.C.Barnes and R.D.Milroy; to be published in Physics of Fluids
13) G.L.Kulcinski, et.al.; Fusion Technology vol.15 (1989) 1233
14) H.L.Berk, H.Momota, and T.Tajima; Physics of Fluids vol.30 (1988) 3024
15) S.P.Auerbach and W.C.Condit; Nuclear Fusion vol.21 (1981) 927
16) H.Momota et al.; Fusion Technology vol.2 (1984) 1463
17) R.W.Moir and W.I.Barr; Nuclear Fusion vol.13 (1973) 35
18) H.Momota; LA-11808-C (Los Alamos, May 1990) 8; Details will be published
19) D.W.Fry, R.B.R.S.Harvie, L.B.Mullett, and W.Walkinshaw; Nature vol.160 (1947) 351
20) B.G.Logan et al.; IAEA CN-50/G-I-5 (Held at Nice, 1988)
21) L.J.Wittenberg, J.F.Santarius, and G.L.Kulcinski; Fusion Technology vol.10 (1986) 167
22) J.P.Holdren, chair; Summary of the Report of the Senior Committee on Environmental, Safety, and Economic Aspects of Magnetic Fusion Energy, UCRL-53766-Summary (1987)
23) H.Momota, M.Ohnishi, and Y.Tomita; Under preparation for publication, also refer LA-11808-C (Los Alamos, May 1990) 44 and 48
24) M.Ohnishi, A.Ishida, and H.Momota; submitted to Physics of Fluids B
25) Y.Ohara et al.; JAERI-M 90-154 (1990)

Phase	a	b	c
Plasma Radius (m)	0.7	1.0	1.12
Plasma Length (m)	4.8	14.8	17.0
Plasma Temperature (keV)	1.0	1.0	87.5
Electron Density ($*10^{20}/m^3$)	4.1	0.62	6.6
Trapped Flux (Wb)	0.086	0.086	3.66
External Magnetic Field (T)	0.56	0.22	6.7
s-Value	5.9	2.7	9.2
Plasma Beta-Value	0.92	0.83	0.90

Table 1: Plasma parameters at the phases
a: after the formation of the FRC
b: after the translation of the FRC
c: steady burning state

Fusion Power: 1,610 MW	
Charged Particles:	1,180 MW
Neutron:	77 MW
Radiation	357 MW
Electric Power: 1,052 MW	
through Direct Energy Converters:	808 MW
through Turbine-Motor Generators:	244 MW
Fusion Plasma	
Volume:	(r_s=1.12m, l_s=17m) 67 m^3
Fuels:	D, ^3He; $n3_{He}:n_d$ = 1:2
Averaged Electron Density:	$6.6*10^{20}/m^3$
Temperature (T_i = T_e)	87.5keV
Beta-Value	90 %
Chamber	
Formation Chamber: r=1.8m, L=15m, t=0.15 Alumina Tube	
Burning Chamber: r=2.0m, L=25m, t=0.05m Ferritic Steel	
Heat Load on the First Wall:	1.70 MW/m^2
14MeV Neutron Load on the First Wall:	0.26 MW/m^2
Energy Conversion Chamber: r=10m, L=50m SS Vessel	
Magnetic Coils	
Pinch Coils: r=2m, L=10m 5-stage tandem, Cu, L_c=1.6μH	
Pulse Coils: r=5m, NbTi/Cu/CuNi, Max 200T/sec 4T, 1.87MAT*8	
Slow Coils: r=3m, NbTi/Cu/CuNi, Max 7T, 14.2MAT*10	
Heating and Current Drive: NBI	
Start Up: Max 1400 keV, 100 MW, D^0 Injection	
Steady Burning: 1000 keV, 5 MW, D^0 Injection	
Fueling: Packman Method, Liq. ^3He in Iced D Vessel	
Deuterium:	56.4 kg/year
Helium-3:	38.0 kg/year

Table 2: Principal parameters of the D-^3He FRC fusion reactor "ARTEMIS"

Capital Cost	146.0 M$/y	0.0844*(99)
Operation and Maintenance	34.6 M$/y	0.020*(99)
Fuel Cost	8.0 M$/y	0.20M$/kg*40kg/y
Total Cost(TAC)	188.6 M$/y	
Cost of Electricity (Capacity Factor:75%)	28.7 mill/kWh	TAC/(8760h/y*0.75*1GW)

Table 3: Cost of electricity with "ARTEMIS"

Fusion Power:	1.6 GW	
Carried by		
14.7MeV Protons		368 MW
Neutrons		77 MW
Thermal Ions		770 MW
Radiation		357 MW
Other Fusion Products		43 MW
Plasma Volume:	67.0 m^3	
Radius		1.12 m
Length		17.0 m
Number Density of Electron:	$6.6*10^{20}/m^3$	
Deuterium		$2.9*10^{20}/m^3$
Helium-3		$1.4*10^{20}/m^3$
Others		$0.6*10^{20}/m^3$
Fueling:	$7.8*10^{21}$/sec	
Pellet Injection		$7.77*10^{21}$/sec
Neutral Beam Injection		$3.1*10^{19}$/sec
Plasma Temperature	87.5 keV	
Current Drive	1 MeV * 5 A (NBI)	
Energy Confinement Time:	2.09 sec	
Particle Confinement Time:	4.18 sec	
External Magnetic Field:	6.7 T	
Beta Value:	0.90	

Table 4: Plasma parameters of a steady burning D-^{3}He FRC

	a	b	c
Inner Radius (m)	2.0	4.75	3.25
Outer Radius (m)	2.2	5.25	3.75
Length of a Coil (m)	0.8	0.5	1.0
Number of Coils	7	8	10
Total Length (m)	10	12	30
Cable	Cu	NbTi SC Strand	NbTi SC Monolith
Total Current•Turns	4MA•1	15MAT	142MAT
Maximum Field	0.56T	4.0T	7.1T
Period	10μsec	20T/s DC	DC

Table 5: Characteristics of magnetic coils
a: Pinch coils for FRC formation
b: Fast coils for guide field in the formation chamber
c: Slow coils for FRC confinement

stage #	1	2	3	4	5
Separation between Fin Array (m)	0.34	0.32	0.39	0.52	0.79
Length of Ion Collector (m)	0.66	0.62	0.61	0.62	1.0
Applied Voltage (kV)	132	245	394	607	954
Obtained Electricity (MW)	45.8	53.8	51.9	39.8	28.6

Distance between Ion Collector Plates:	0.25m
Tickness of Ion Collector Plate:	0.012m
Angle between Arrays and Lines of Force:	0.044radian
Total Length of the Assembly:	2.2m
Radius of the Assembly:	2m
Efficiency of the Converter:	60.8%

Table 6: Applied voltage and the size of the ion collectors

Acc.#	Description	Cost(M$)			Mass(tons). Unit Cost. Scale
20	Land	5.0			
21	Building and Site Facilities	196.9			
212	Reactor building	132.2		3.0	$118.6*(V/2.5)^{0.67}$
213	Turbine building	14.8		244.0	$35.92*(Pt/1440)^{0.50}$
214	Reactor maintenance building	49.8		1000MWe	
22	Reactor plant equipment	520.4			
221	Reactor system	404.4			
2211	Vacuum vessel/First wall	12.9			
22111	Formation chamber		3.2	105	Alumina 30$/kg
			0.3	10.5	SS 25$/kg
22112	Burning chamber		9.5	189	HT 50$/kg
2212	Shield	20.6		589	SS+B4C 35$/kg
2213	Magnet system	56.4		3.0	$118.6*(V/2.5)^{0.67}$
22131	SC magnet	55.0			
			(33.0)	1000	NbTi/Cu 33.3$/kg
			(2.1)	60	SS can 34.6$/kg
			(19.9)	600	SS support 33.2$/kg
22132	Pinch coil		1.4	100	Cu 14$/kg
2214	Heating system (NBI)	225.0		100MW	NBI 2.25$/W
2215	Structure	8.0			
2216	Vacuum vessel pumping system	4.0			
2217	Power plant and capacitor banks	15.5		33MW	0.47M$/MJ
2218	Direct energy converter	62.0			
			0.2	3.1	grid 50$/kg
			12.0	600	chamber 20$/kg
			49.8	808MW	electric equipment
222	Main cooling system	28.4		678MW	$93.1*(Pth/4000)^{0.67}$
223	Auxiliary cooling system	10.8		1610MW	$19.8*(Pf/4000)^{0.67}$
224	Radioactive waste facility	0.5		77MW	$6.4*(Pn/4000)^{0.67}$
225	Plasma fueling system	27.9		1610MW	$51.3*(Pf/4000)^{0.67}$
226	Other plant equipments	31.6		1610MW	$58.2*(Pf/4000)^{0.67}$
228	Instrumentation and control	16.9		1610MW	$31.1*(Pf/4000)^{0.67}$
23	Turbine plant equipment	82.2		244MW	$332.5*(Pth/1400)^{0.8}$
24	Electrical equipment	143.2		1052MW	$161.2*(Pe/1400)^{0.4}$
25	Misc. plant equipment	59.6		1000MW	$69.2*(Pnet/1200)^{0.3}$
90	Total direct cost	1,007.8			
91-93	Indirect cost	585.6			0.581*(90)
94	Interest during construction	136.4			0.0856*(90+91)
99	Total plant capital cost	1,729.8			

Table.7: The constitution of the total plant capital cost: The following financial assumptions have been introduced,i.e., interest during construction = 0.0856, plant life time = 30years, and indirect cost factor = 0.581, and the capacity factor = 0.75.

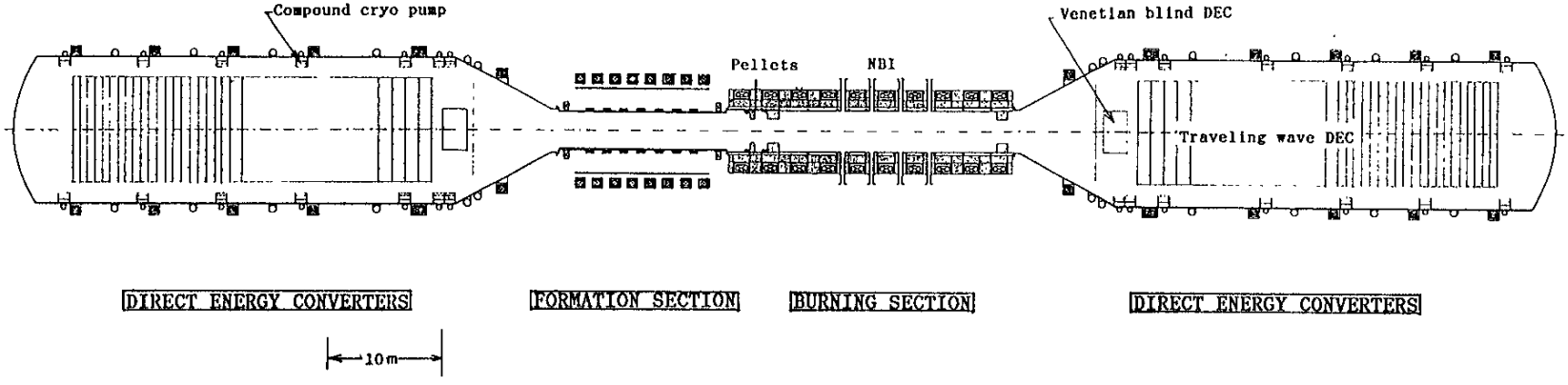

Fig.1: A whole view of the D-^{3}He FRC reactor "ARTEMIS" composed of formation chamber, burning chamber, and direct energy converters

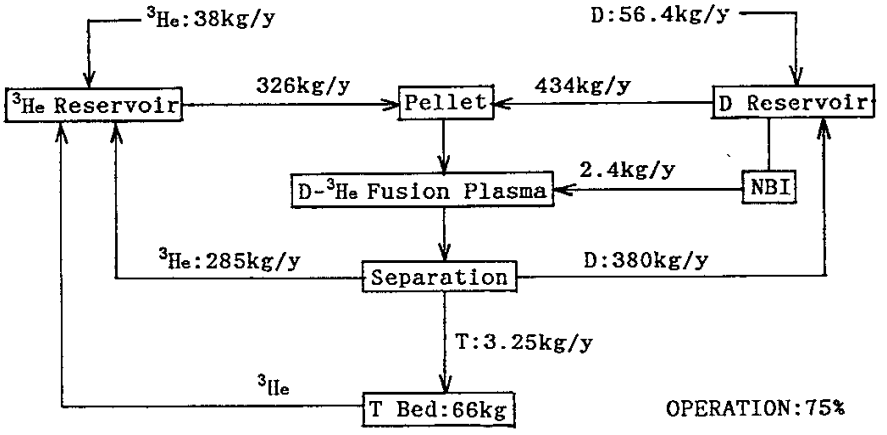

Fig.2: A chart of particles flows in "ARTEMIS": A certain part of fusion particles are lost directly and others are diffused out of plasma.

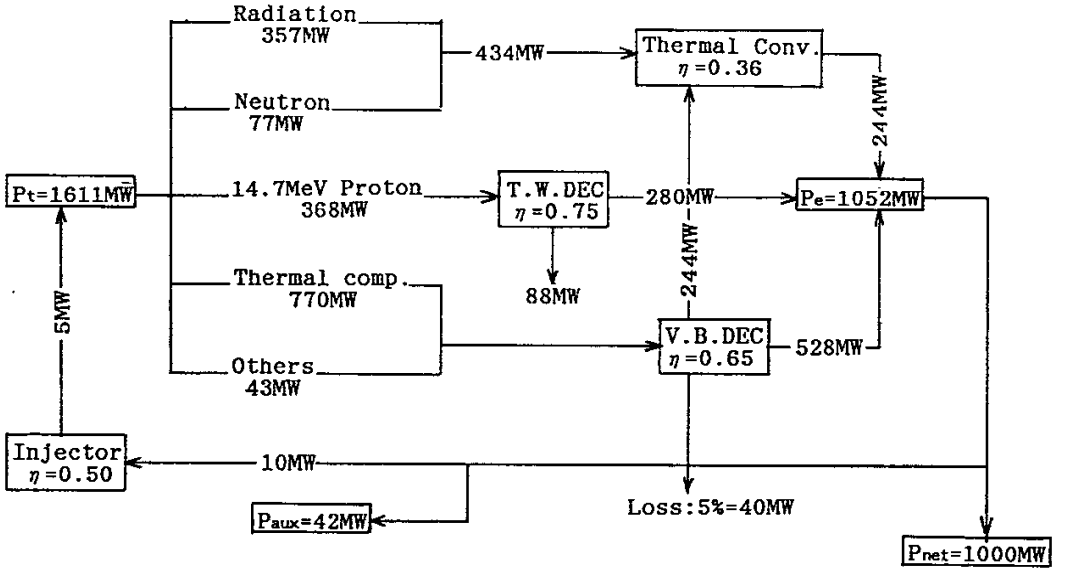

Fig.3: A power flow diagram of D-^{3}He FRC power plant "ARTEMIS": On the bases of high efficiency of the direct energy converters, an overall plant efficiency is as high as 62%.

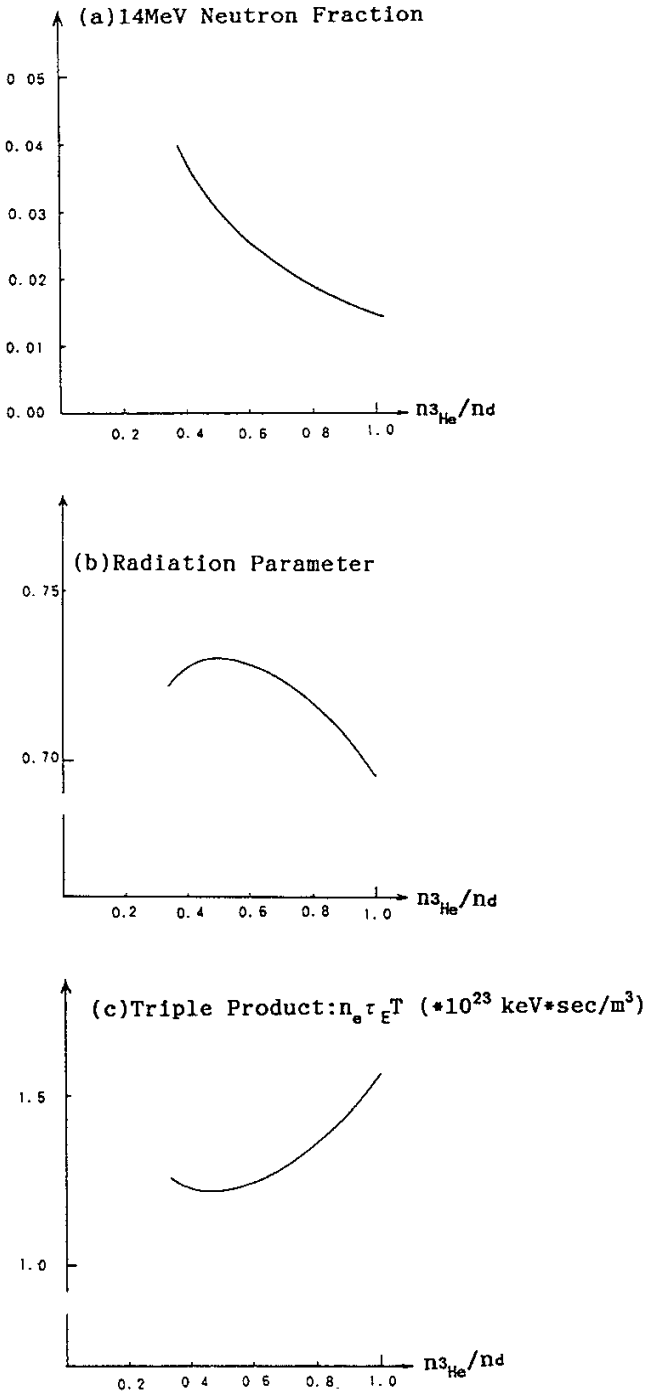

Fig.4: (a) The 14MeV neutron power fraction, (b) The radiation parameter, and (c) The triple product $n_e \tau_E T$ versus the concentration of Helium-3 and deuterium: Plasma temperature of 90keV and averaged beta-value of 90% are assumed. The ratio of the particles confinement time and the energy confinement time is also assumed to be 2.

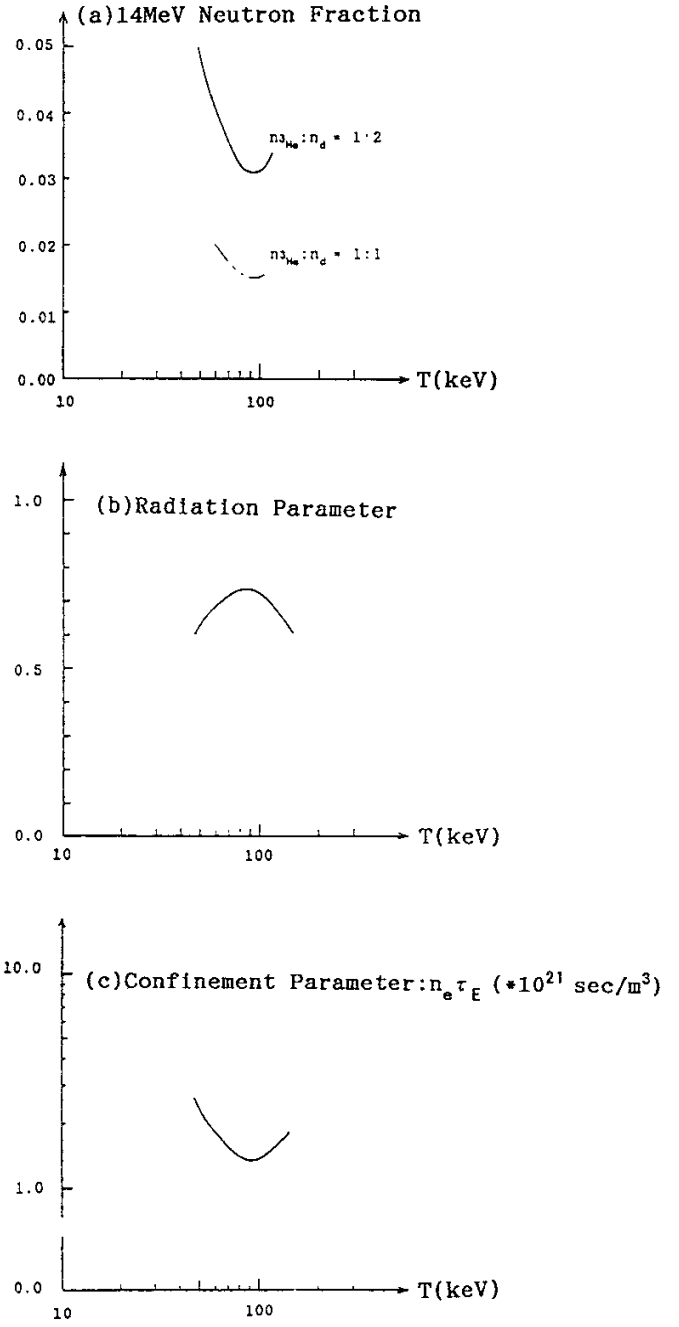

Fig.5: (a) 14MeV neutron fraction, (b) The radiation parameter, and (c) The confinement parameter $n_e\tau_E$ of D-^{3}He fusion plasma versus the operation temperature: In Figs. 5-a, b, and c, averaged beta-value is still assumed to be 90% and the helium-3 density is chosen as 1/2 of the deuterium density. The particles confinement time is assumed to be twice of the energy confinement time.

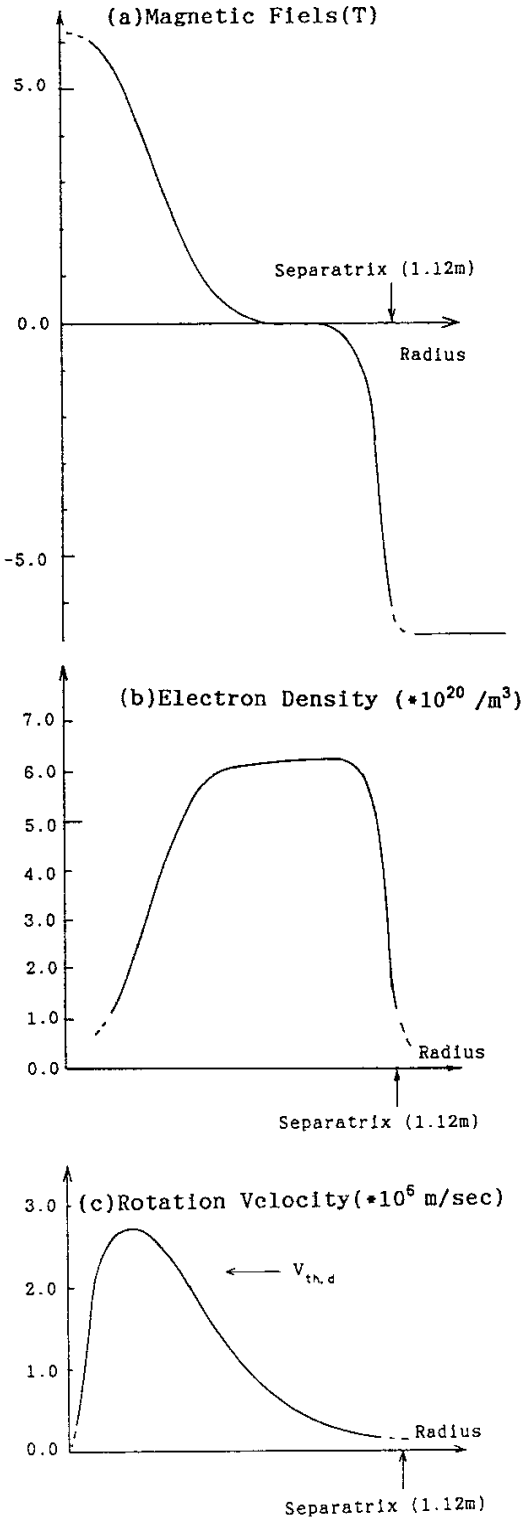

Fig.6: A steady state equilibrium at the midplane of the burning FRC plasma: (a) The magnetic field, (b) The electron density, and (c) The rotation velocity

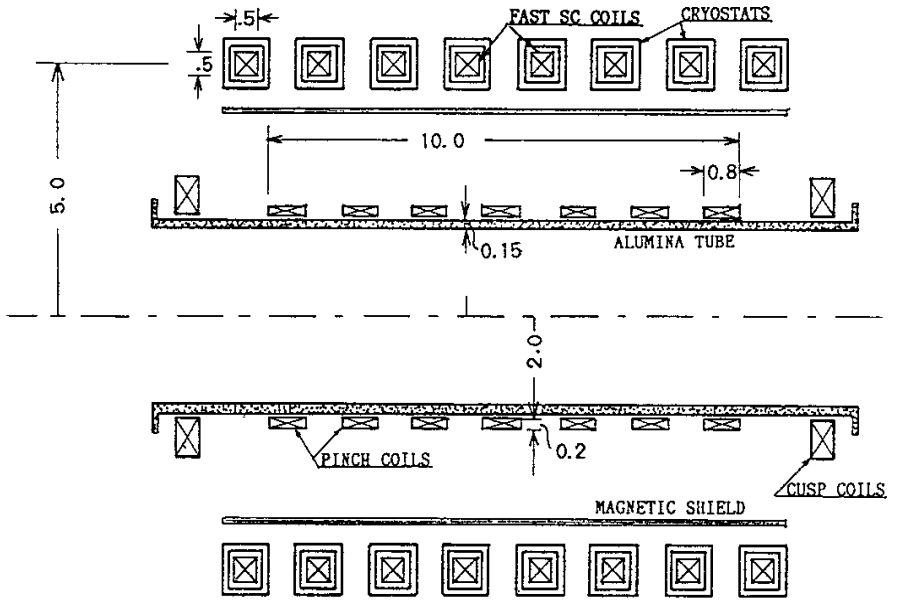

Fig.7: A cross-section of the formation chamber, which consists of a set of pinch coils for the FRC formation, a set of fast coils for a guide field, and two cusp coils operated together with pinch coils.

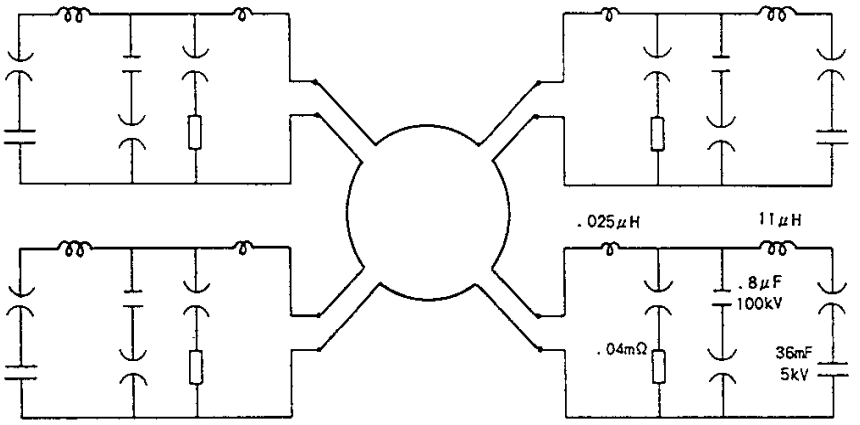

Fig.8: The electric circuits for 4-stage tandem pinch coils.

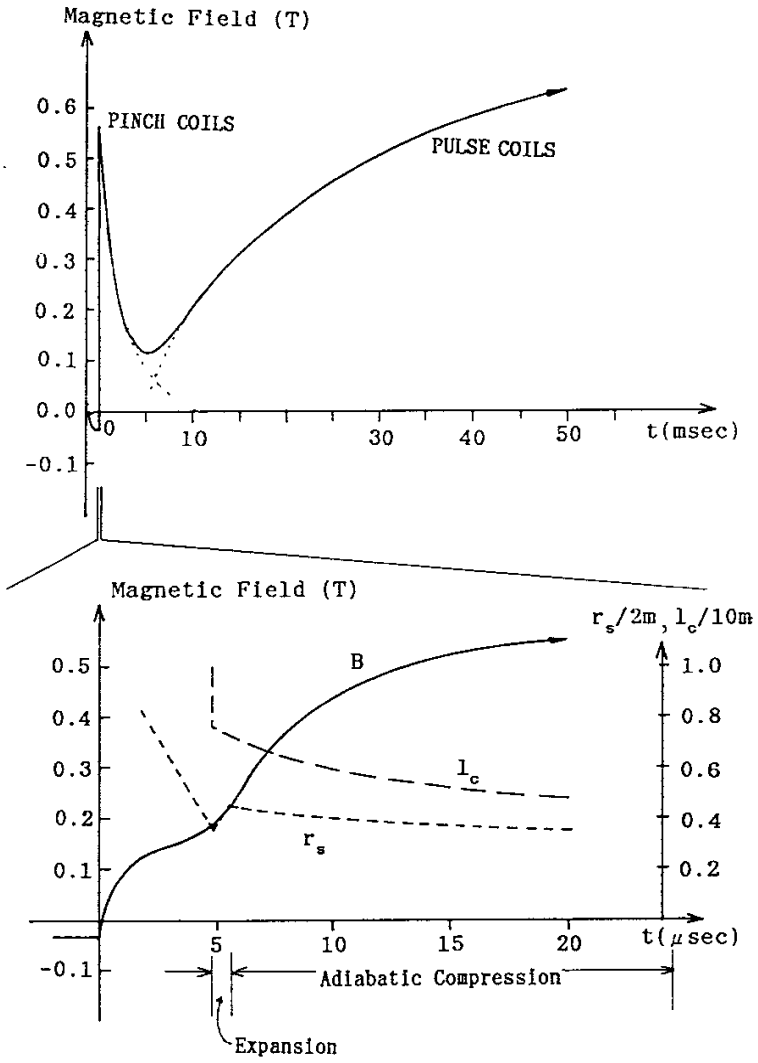

Fig.9: The time sequence of applied external magnetic fields, the separatrix radius r_s, and the length l_s of the obtained FRC.

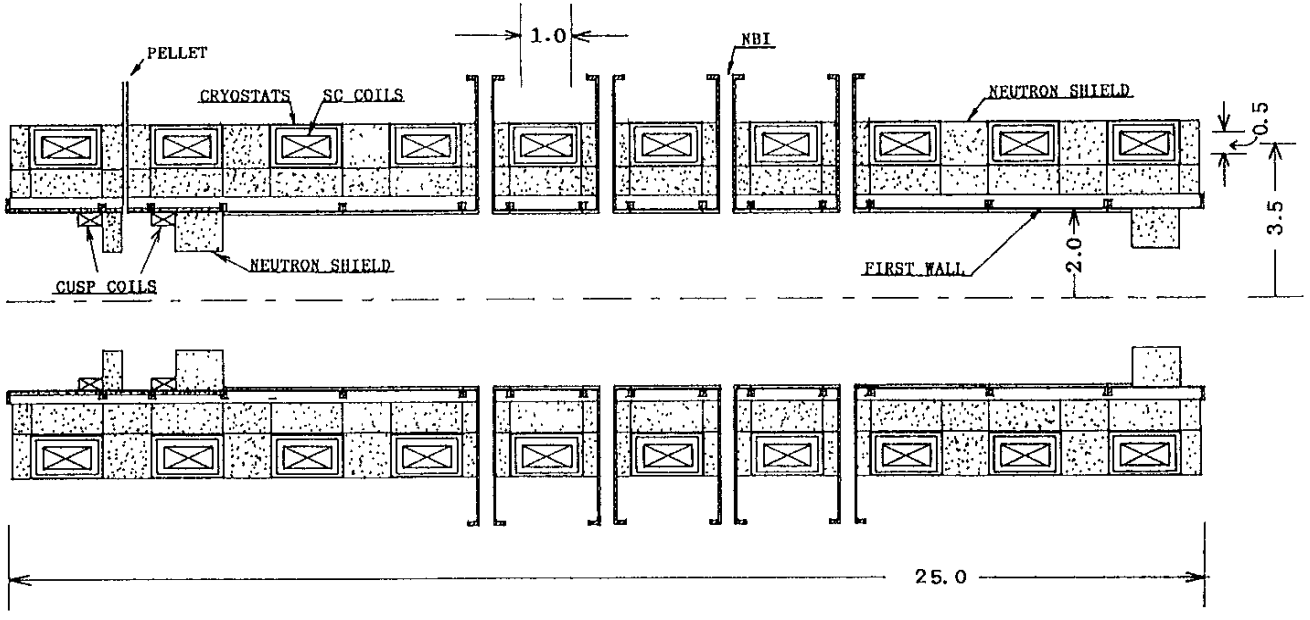

Fig.10: A Cross-sectional drawing of the burning section

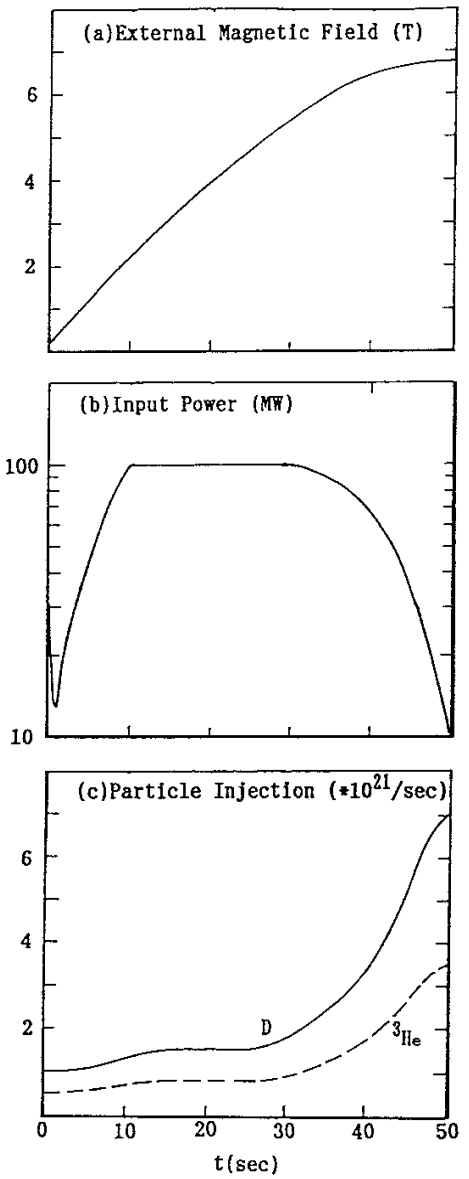

Fig.11: (a) The applied external magnetic field
(b) The input NBI power
(c) The injected number of the particles with pellet per second

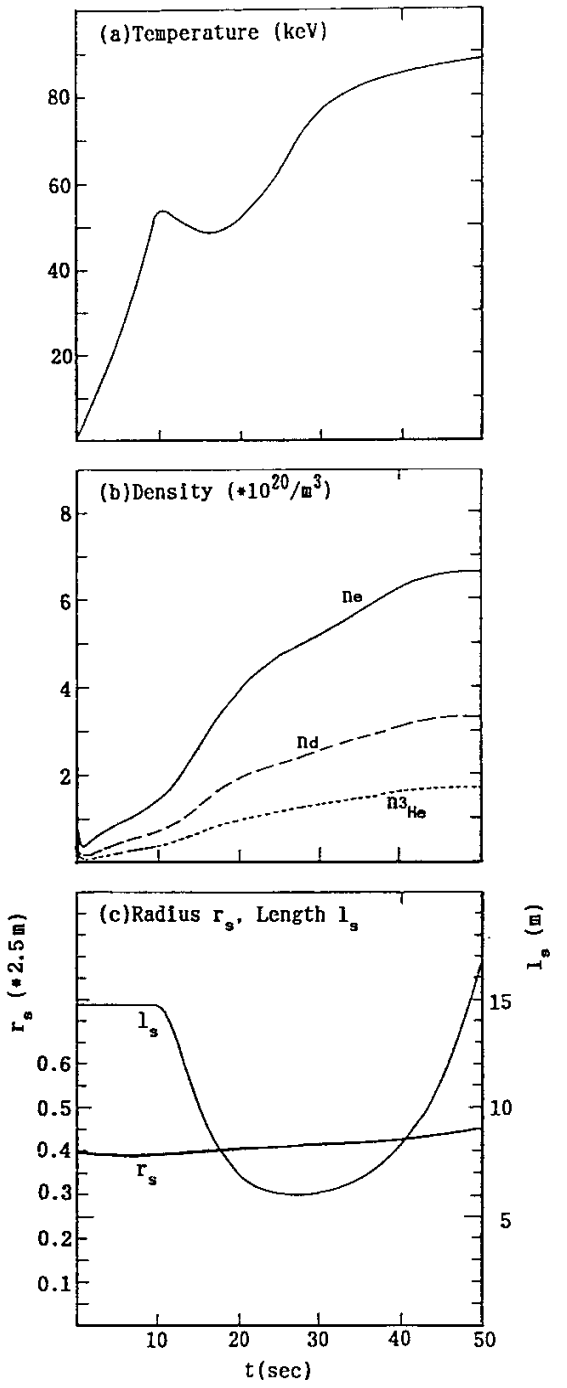

Fig.12: A development of plasma attributed to the injections(Fig.11): (a) temperature, (b) averaged density, and(c) radius and length

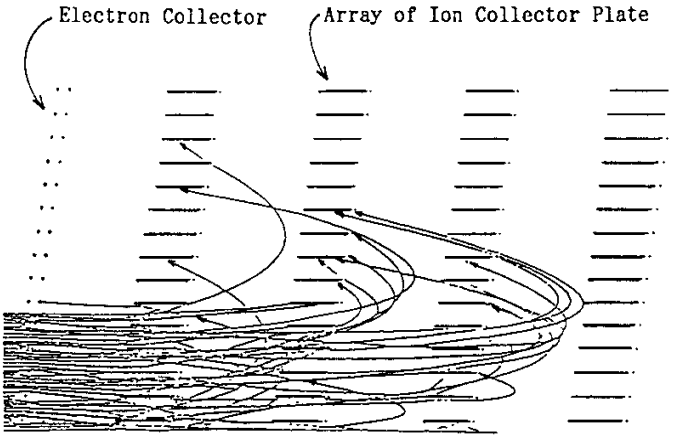

Fig.13: Examples of orbits of thermal ^{3}He ions at the Venetian blind direct energy converter

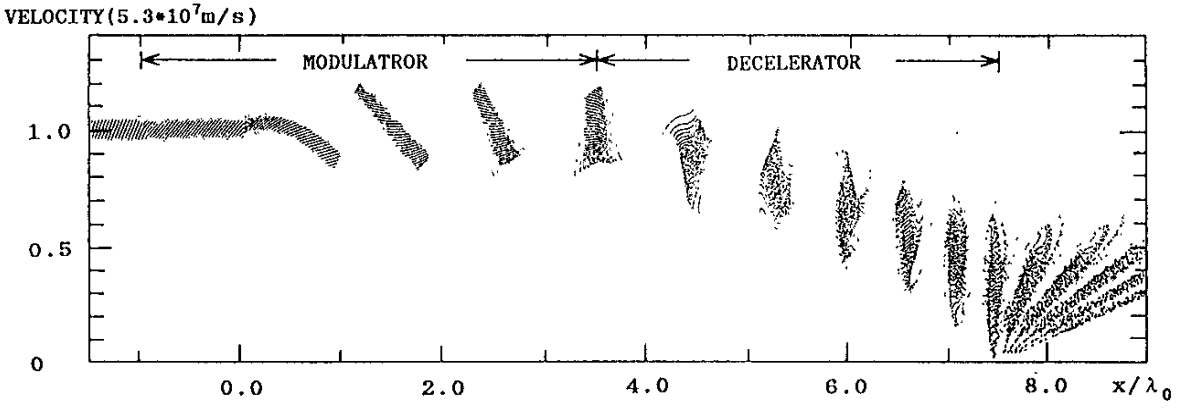

Fig.14: Phase space plotts of fusion protons; Applied maximum voltage at the modulator and the entrance of the decelerator is respectively 0.82MV and 1.05MV. 95% of protons are trapped and decelerated.

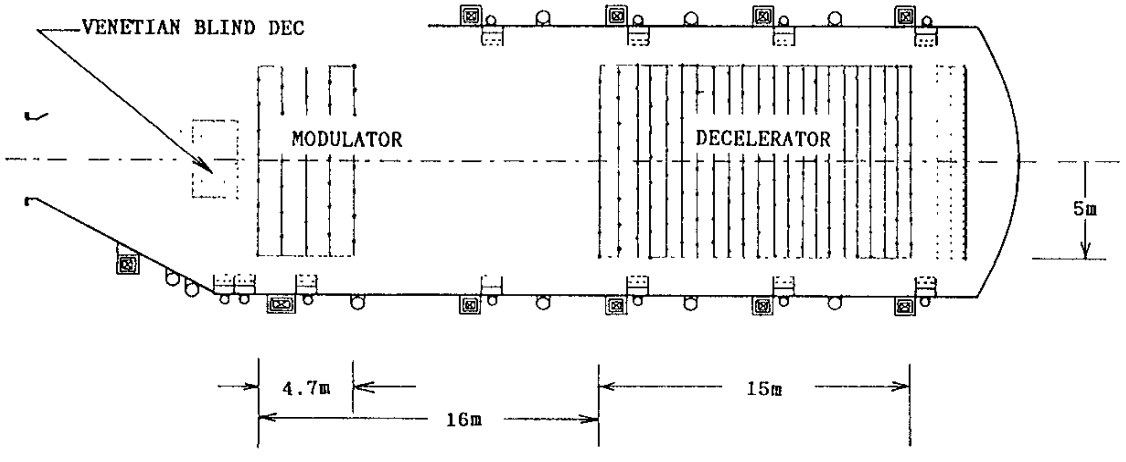

Fig 15: Assembly of a traveling wave direct energy converter

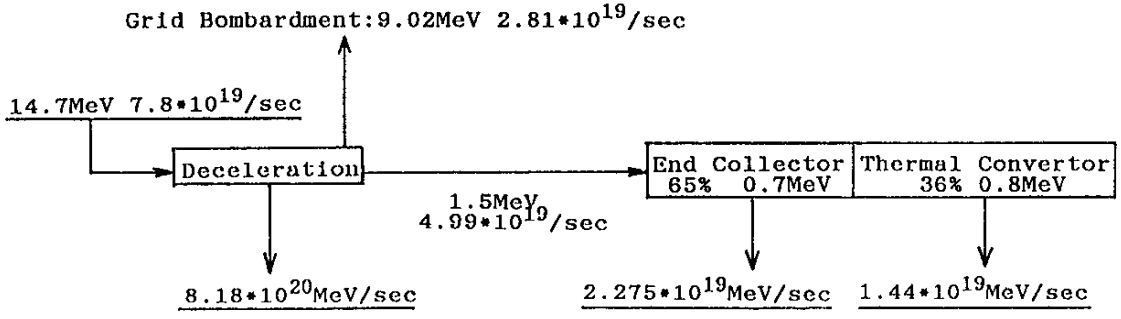

Efficiency:75%

Fig.16: An energy flow chart of the traveling wave direct energy converter

Recent Issues of NIFS Series

NIFS-44 T.Hayashi, A.Takei, N.Ohyabu, T.Sato, M.Wakatani, H.Sugama, M.Yagi, K.Watanabe, B.G.Hong and W.Horton, *Equilibrium Beta Limit and Anomalous Transport Studies of Helical Systems*; Sep. 1990

NIFS-45 R.Horiuchi, T.Sato, and M.Tanaka, *Three-Dimensional Particle Simulation Study on Stabilization of the FRC Tilting Instability*; Sep. 1990

NIFS-46 K.Kusano, T.Tamano and T. Sato, *Simulation Study of Nonlinear Dynamics in Reversed-Field Pinch Configuration*; Sep. 1990

NIFS-47 Yoshi H.Ichikawa, *Solitons and Chaos in Plasma*; Sep. 1990

NIFS-48 T.Seki, R.Kumazawa, Y.Takase, A.Fukuyama, T.Watari, A.Ando, Y.Oka, O.Kaneko, K.Adati, R.Akiyama, R.Ando, T.Aoki, Y.Hamada, S.Hidekuma, S.Hirokura, K.Ida, K.Itoh, S.-I.Itoh, E.Kako, A. Karita, K.Kawahata, T.Kawamoto, Y.Kawasumi, S.Kitagawa, Y.Kitoh, M.Kojima, T.Kuroda, K.Masai, S.Morita, K.Narihara, Y.Ogawa, K.Ohkubo, S.Okajima, T.Ozaki, M.Sakamoto, M.Sasao, K.Sato, K.N.Sato, F.Shinbo, H.Takahashi, S.Tanahashi, Y.Taniguchi, K.Toi and T.Tsuzuki, *Application of Intermediate Frequency Range Fast Wave to JIPP T-IIU Plasma*; Sep.1990

NIFS-49 A.Kageyama, K.Watanabe and T.Sato, *Global Simulation of the Magnetosphere with a Long Tail: The Formation and Ejection of Plasmoids*; Sep.1990

NIFS-50 S.Koide, *3-Dimensional Simulation of Dynamo Effect of Reversed Field Pinch*; Sep. 1990

NIFS-51 O.Motojima, K. Akaishi, M.Asao, K.Fujii, J.Fujita, T.Hino, Y.Hamada, H.Kaneko, S.Kitagawa, Y.Kubota, T.Kuroda, T.Mito, S.Morimoto, N.Noda, Y.Ogawa, I.Ohtake, N.Ohyabu, A.Sagara, T. Satow, K.Takahata, M.Takeo, S.Tanahashi, T.Tsuzuki, S.Yamada, J.Yamamoto, K.Yamazaki, N.Yanagi, H.Yonezu, M.Fujiwara, A.Iiyoshi and LHD Design Group, *Engineering Design Study of Superconducting Large Helical Device*; Sep. 1990

NIFS-52 T.Sato, R.Horiuchi, K. Watanabe, T. Hayashi and K.Kusano, *Self-Organizing Magnetohydrodynamic Plasma*; Sep. 1990

NIFS-53 M.Okamoto and N.Nakajima, *Bootstrap Currents in Stellarators and Tokamaks*; Sep. 1990

NIFS-54 K.Itoh and S.-I.Itoh, *Peaked-Density Profile Mode and Improved Confinement in Helical Systems*; Oct. 1990

NIFS-55 Y.Ueda, T.Enomoto and H.B.Stewart, *Chaotic Transients and Fractal Structures Governing Coupled Swing Dynamics*; Oct. 1990

NIFS-56 H.B.Stewart and Y.Ueda, *Catastrophes with Indeterminate Outcome*; Oct. 1990

NIFS-57 S.-I.Itoh, H.Maeda and Y.Miura, *Improved Modes and the Evaluation of Confinement Improvement*; Oct. 1990

NIFS-58 H.Maeda and S.-I.Itoh, *The Significance of Medium- or Small-size Devices in Fusion Research*; Oct. 1990

NIFS-59 A.Fukuyama, S.-I.Itoh, K.Itoh, K.Hamamatsu, V.S.Chan, S.C.Chiu, R.L.Miller and T.Ohkawa, *Nonresonant Current Drive by RF Helicity Injection*; Oct. 1990

NIFS-60 K.Ida, H.Yamada, H.Iguchi, S.Hidekuma, H.Sanuki, K.Yamazaki and CHS Group, *Electric Field Profile of CHS Heliotron/Torsatron Plasma with Tangential Neutral Beam Injection*; Oct. 1990

NIFS-61 T.Yabe and H.Hoshino, *Two- and Three-Dimensional Behavior of Rayleigh-Taylor and Kelvin-Helmholz Instabilities*; Oct. 1990

NIFS-62 H.B. Stewart, *Application of Fixed Point Theory to Chaotic Attractors of Forced Oscillators;* Nov. 1990

NIFS-63 K.Konn., M.Mituhashi, Yoshi H.Ichikawa,*Soliton on Thin Vortex Filament;* Dec. 1990

NIFS-64 K.Itoh, S.-I.Itoh and A.Fukuyama,*Impact of Improved Confinement on Fusion Research;* Dec. 1990

NIFS -65 A.Fukuyama, S.-I.Itoh and K. Itoh,*A Consistency Analysis on the Tokamak Reactor Plasmas;* Dec. 1990

NIFS-66 K.Itoh, H. Sanuki, S.-I. Itoh and K. Tani,*Effect of Radial Electric Field on α-Particle Loss in Tokamaks;* Dec. 1990

NIFS-67 K.Sato,and F.Miyawaki,*Effects of a Nonuniform Open Magnetic Field on the Plasma Presheath*; Jan.1991

NIFS-68 K.Itoh and S.-I.Itoh,*On Relation between Local Transport Coefficient and Global Confinement Scaling Law;* Jan. 1991

NIFS-69 T.Kato, K.Masai, T.Fujimoto,F.Koike, E.Källne, E.S.Marmar and J.E.Rice,*He-like Spectra Through Charge Exchange Processes in Tokamak Plasmas;* Jan.1991

NIFS-70 K. Ida, H. Yamada, H. Iguchi, K. Itoh and CHS Group, *Observation of Parallel Viscosity in the CHS Heliotron/Torsatron* ; Jan.1991

NIFS-71 H. Kaneko, *Spectral Analysis of the Heliotron Field with the Toroidal Harmonic Function in a Study of the Structure of Built-in Divertor* ; Jan. 1991

NIFS-72 S. -I. Itoh, H. Sanuki and K. Itoh, *Effect of Electric Field Inhomogeneities on Drift Wave Instabilities and Anomalous Transport* ; Jan. 1991

NIFS-73 Y.Nomura, Yoshi.H.Ichikawa and W.Horton, *Stabilities of Regular Motion in the Relativistic Standard Map*; Feb. 1991

NIFS-74 T.Yamagishi, *Electrostatic Drift Mode in Toroidal Plasma with Minority Energetic Particles,* Feb. 1991

NIFS-75 T.Yamagishi, *Effect of Energetic Particle Distribution on Bounce Resonance Excitation of the Ideal Ballooning Mode,* Feb. 1991

NIFS-76 T.Hayashi, A.Tadei, N.Ohyabu and T.Sato, *Suppression of Magnetic Surface Breading by Simple Extra Coils in Finite Beta Equilibrium of Helical System;* Feb. 1991

NIFS-77 N. Ohyabu, *High Temperature Divertor Plasma Operation*; Feb. 1991

NIFS-78 K.Kusano, T. Tamano and T. Sato, *Simulation Study of Toroidal Phase-Locking Mechanism in Reversed-Field Pinch Plasma*; Feb. 1991

NIFS-79 K. Nagasaki, K. Itoh and S. -I. Itoh, *Model of Divertor Biasing and Control of Scrape-off Layer and Divertor Plasmas*; Feb. 1991

NIFS-80 K. Nagasaki and K. Itoh, *Decay Process of a Magnetic Island by Forced Reconnection*; Mar. 1991

NIFS-81 K. Takahata, N. Yanagi, T. Mito, J. Yamamoto, O.Motojima and LHDDesign Group, K. Nakamoto, S. Mizukami, K. Kitamura, Y. Wachi, H. Shinohara, K. Yamamoto, M. Shibui, T. Uchida and K. Nakayama, *Design and Fabrication of Forced-Flow Coils as R&D Program for Large Helical Device*; Mar. 1991

NIFS-82 T. Aoki and T. Yabe, *Multi-dimensional Cubic Interpolation for ICF Hydrodynamics Simulation*; Apr. 1991

NIFS-83 K. Ida, S.-I. Itoh, K. Itoh, S. Hidekuma, Y. Miura, H. Kawashima, M. Mori, T. Matsuda, N. Suzuki, H. Tamai, T.Yamauchi and JFT-2M Group, *Density Peaking in the JFT-2M Tokamak Plasma with Counter Neutral Beam Injection* ; May 1991

NIFS-84 A. Iiyoshi, *Development of the Stellarator/Heliotron Research*; May 1991

NIFS-85 Y. Okabe, M. Sasao, H. Yamaoka, M. Wada and J. Fujita, *Dependence of Au^- Production upon the Target Work Function in a Plasma-Sputter-Type Negative Ion Source;* May 1991

NIFS-86 N. Nakajima and M. Okamoto, *Geometrical Effects of the Magnetic Field on the Neoclassical Flow, Current and Rotation in General Toroidal Systems*; May 1991

NIFS-87 S. -I. Itoh, K. Itoh, A. Fukuyama, Y. Miura and JFT-2M Group, *ELMy-H mode as Limit Cycle and Chaotic Oscillations in Tokamak Plasmas;* May 1991

NIFS-88 N.Matsunami and K.Kitoh, *High Resolution Spectroscopy of H^+ Energy Loss in Thin Carbon Film;* May 1991

NIFS-89 H. Sugama, N. Nakajima and M.Wakatani, *Nonlinear Behavior of Multiple-Helicity Resistive Interchange Modes near Marginally Stable States;* May 1991

NIFS-90 H. Hojo and T.Hatori, *Radial Transport Induced by Rotating RF Fields and Breakdown of Intrinsic Ambipolarity in a Magnetic Mirror*; May 1991

NIFS-91 M. Tanaka, S. Murakami, H. Takamaru and T.Sato, *Macroscale Implicit, Electromagnetic Particle Simulation of Inhomogeneous and Magnetized Plasmas in Multi-Dimensions;* May 1991

NIFS-92 S. - I. Itoh, *H-mode Physics, -Experimental Observations and Model Theories-, Lecture Notes, Spring College on Plasma Physics, May 27 - June 21 1991 at International Centre for Theoretical Physics (IAEA UNESCO) Trieste, Italy ;* Jun. 1991

NIFS-93 Y. Miura, K. Itoh, S. - I. Itoh, T. Takizuka, H. Tamai, T. Matsuda, N. Suzuki, M. Mori, H. Maeda and O. Kardaun, *Geometric Dependence of the Scaling Law on the Energy Confinement Time in H-mode Discharges;* Jun. 1991

NIFS-94 H. Sanuki, K. Itoh, K. Ida and S. - I. Itoh, *On Radial Electric Field Structure in CHS Torsatron / Heliotron;* Jun. 1991

NIFS-95 K. Itoh, H. Sanuki and S. - I. Itoh, *Influence of Fast Ion Loss on Radial Electric Field in Wendelstein VII-A Stellarator;* Jun. 1991

NIFS-96 S. - I. Itoh, K. Itoh, A. Fukuyama, *ELMy-H mode as Limit Cycle and Chaotic Oscillations in Tokamak Plasmas;* Jun. 1991

NIFS-97 K. Itoh, S. - I. Itoh, H. Sanuki, A. Fukuyama, *An H-mode-Like Bifurcation in Core Plasma of Stellarators;* Jun. 1991

NIFS-98 H. Hojo, T. Watanabe, M. Inutake, M. Ichimura and S. Miyoshi, *Axial Pressure Profile Effects on Flute Interchange Stability in the Tandem Mirror GAMMA 10;* Jun. 1991

NIFS-99 A. Usadi, A. Kageyama, K. Watanabe and T. Sato, *A Global Simulation of the Magnetosphere with a Long Tail : Southward and Northward IMF;* Jun. 1991

NIFS-100 H. Hojo, T. Ogawa and M. Kono, *Fluid Description of Ponderomotive Force Compatible with the Kinetic One in a Warm Plasma* ; July 1991